Accepted Manuscript

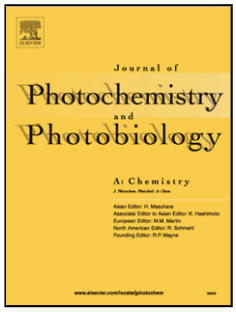

Title: A PHOTOPHYSICAL AND SPECTROELECTROCHEMICAL STUDY ON N-PHENYL-CARBAZOLES AND THEIR OXIDIZED SPECIES

Authors: Cristina Luján Ramírez, María Inés Mangione, Sonia Graciela Bertolotti, Ernesto Maximiliano Arbeloa, Alejandro Rubén Parise

PII: S1010-6030(18)30990-0
DOI: https://doi.org/10.1016/j.jphotochem.2018.07.039
Reference: JPC 11405

To appear in: *Journal of Photochemistry and Photobiology A: Chemistry*

Received date: 10-7-2018
Revised date: 23-7-2018
Accepted date: 25-7-2018

Please cite this article as: Ramírez CL, Mangione MI, Bertolotti SG, Arbeloa EM, Parise AR, A PHOTOPHYSICAL AND SPECTROELECTROCHEMICAL STUDY ON N-PHENYL-CARBAZOLES AND THEIR OXIDIZED SPECIES, *Journal of Photochemistry and amp; Photobiology, A: Chemistry* (2018), https://doi.org/10.1016/j.jphotochem.2018.07.039

This is a PDF file of an unedited manuscript that has been accepted for publication. As a service to our customers we are providing this early version of the manuscript. The manuscript will undergo copyediting, typesetting, and review of the resulting proof before it is published in its final form. Please note that during the production process errors may be discovered which could affect the content, and all legal disclaimers that apply to the journal pertain.

ACCEPTED MANUSCRIPT

A PHOTOPHYSICAL AND SPECTROELECTROCHEMICAL STUDY ON N-PHENYL-CARBAZOLES AND THEIR OXIDIZED SPECIES

Cristina Luján Ramírez,[1] María Inés Mangione,[2] Sonia Graciela Bertolotti,[3] Ernesto Maximiliano Arbeloa,[3]* Alejandro Rubén Parise[1]*

[1] Departamento de Química, Facultad de Ciencias Exactas y Naturales, Universidad Nacional de Mar del Plata. Funes 3350, Nivel II, Mar del Plata, Buenos Aires, Argentina. QUIAMM – INBIOTEC – CONICET

[2] Instituto de Química Rosario, Facultad de Ciencias Bioquímicas y Farmacéuticas, Universidad Nacional de Rosario-CONICET, Suipacha 531, S2002LRK Rosario, Argentina

[3] Departamento de Quimica, FCEFQN, Universidad Nacional de Rio Cuarto, Ruta 36 Km 601, Río Cuarto, Córdoba, Argentina. Instituto de Tecnologías Energéticas y Materiales Avanzados (UNRC-CONICET)

Corresponding authors:

*Ernesto M. Arbeloa

e-mail: earbeloa@exa.unrc.edu.ar

*Alejandro R. Parise

e-mail: aparise@mdp.edu.ar

ACCEPTED MANUSCRIPT

ACCEPTED MANUSCRIPT

Graphical abstract

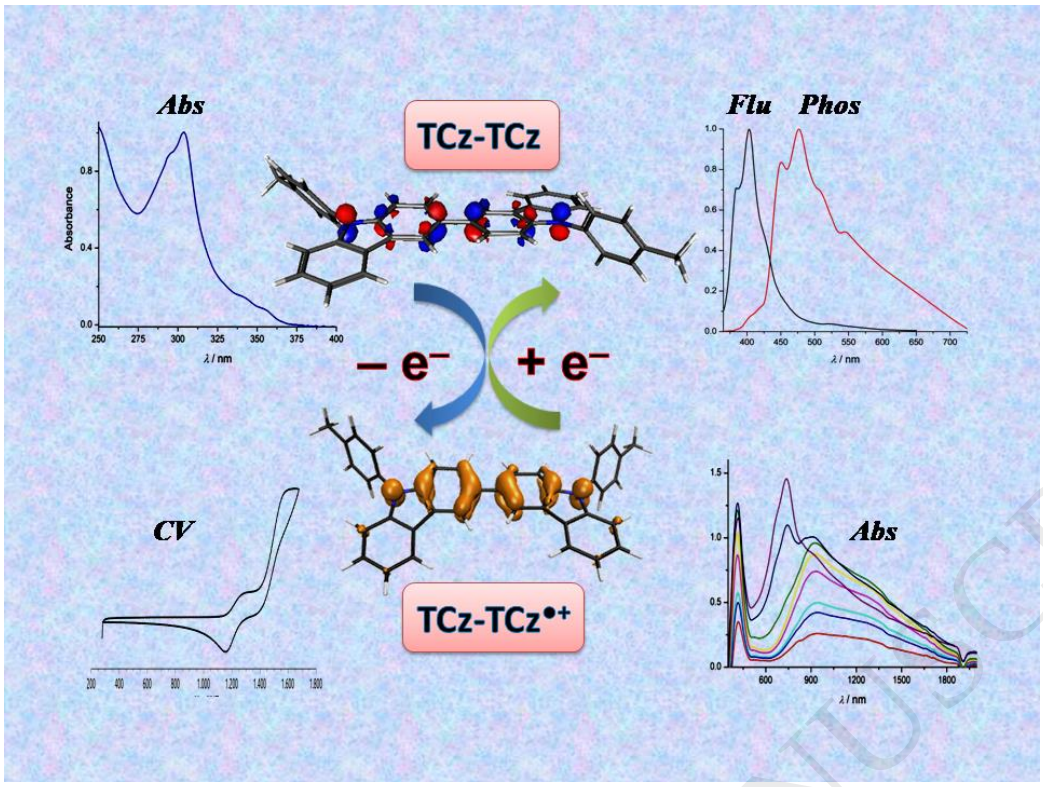

Highlights

- Ground and singlet excited states of N-phenyl-carbazoles were characterized.
- Properties of dicarbazoles are susceptible to electronic coupling between single units.
- The oxidized species were analyzed by cyclic voltammetry and spectroelectrochemistry.
- An electrochromic polymer was deposited by electropolymerization.
- The studied compounds might be suitable as fluorescent sensors and hole transporters.

Abstract

A series of *N*-phenyl-carbazole derivatives namely TCz (*N*-tolyl-carbazol), TCz-TCz (a 3,3´-linked dimer), and CzPh-CH_2-PhCz (a methylene-bridged *N*-phenyl-carbazole), have been synthesized and studied by means of absorption and fluorescence spectra, DFT calculations, cyclic voltammetry and spectroelectrochemistry. It is concluded that the methylene bridge in CzPh-CH_2-PhCz isolates the two TCz units, whereas TCz-TCz allows extending the electronic coupling along both carbazoles. Moreover, the phosphorescence

ACCEPTED MANUSCRIPT

spectrum of TCz-TCz showed a high energy triplet state (2.61 eV). It was observed that oxidation of CzPh-CH_2-PhCz generates an electrochromic polymer containing TCz-TCz dimer units separated by methylene bridges. Oxidized TCz-TCz subunit was analyzed by EPR spectroscopy, and found to be a Class III mixed valence ion in Robin and Day classification. All results suggest that these molecules might be suitable as selective probes in fluorescence sensing or as host materials in electroluminescent devices.

Keywords: Carbazole – Photophysics – Excited states – Mixed valence – Electroluminescent materials

1. Introduction

The study on the photophysical and photochemical properties of carbazole and carbazole derivatives has attracted the attention of many researchers in the last decades due to the implication of these molecules in photoinduced energy- and electron-transfer reactions. After radiation absorption, the photoprocesses that occur from the excited states of carbazole can find applications in areas of increasing current relevance such as sensitizing, sensing chemistry, electrochemistry and optical materials among others.[1-6] Since their relatively simple synthesis procedure and versatility in functionalization, carbazoles are excellent fragments for the design of hole transporters materials because they combine chemical robustness with electronically tunable properties.[7, 8] Nowadays, the use of carbazoles in thermally activated delayed fluorescence (TADF) processes for development of the third generation of OLED technology is a featured topic in the optoelectronic devices field.[9]

Early reports deal with the synthesis and photophysical characterization of various *N*- and *C*-substituted carbazoles.[10-13] The luminescent properties of these compounds were highlighted from the high emission quantum yields obtained. Among the most remarkable studies, the authors assessed the heavy atom effects on the singlet-to-triplet intersystem crossing process from a series of halide-derivatives.[11, 12] Such results were of practical interest in organic synthesis because the triplet excited states of carbazoles promote the heterolytic cleavage of carbon-halide bonds, which leads to reactive fragments capable of forming new C-C bonds with adequate substrates. The synthesis

ACCEPTED MANUSCRIPT

procedure and photophysical and electrochemical characterization of new extended π-systems based on carbazole-chromophore conjugates continue to be subject of constant research, because of their application in optical and functional materials.[14, 15]

Due to the intrinsic fluorescent capacity of carbazoles, several carbazole derivatives have been investigated for application as selective sensors for metal ions, anions and compounds of biological interest in homogeneous solution.[16-18] Recently, studies on the photophysics of several dye-carbazole couples demonstrated the relevance of these chromophoric composites for optical and sensitizing processes.[19-21] For example, a series of dye-carbazole derivatives has been recently synthesized to develop new photoinitiating systems for free radical and cationic polymerizations, taking advantage of their light absorption properties.[22-24] In order to obtain fluorescent nanoparticles for lysosomal bioimaging in living cells, the synthesis and spectroscopic characterization of BODIPY-carbazole dye were also reported.[25]

It is also known that the particular photophysics of carbazole-containing polymers is responsible for its good electron donor capacity and outstanding photoelectrical properties.[26-28] Among carbazole derivatives *N*-phenyl-carbazoles are of particular interest due to display high thermal stabilities and tunable photoluminescence, which directly influences their optical and electric properties.[29, 30] By attaching proper substituents the dihedral angle between *N*-phenyl ring and carbazole moiety can be modified, so affecting the grade of electron delocalization and the energy of the electronic excited states. Furthermore, the pendant *N*-phenyl groups in the carbazole units of copolymers reduce the rigidity and enhance the flexibility along polymer main chains, thus resulting in good polymer solubility. Accordingly, *N*-phenyl-carbazoles are very interesting building blocks to design soluble and thermally stable polymer with light-emitting properties.[31, 32] Recently, new polycarbazole films based on *N*-phenyl derivatives were electrochemically synthesized, which showed good electrochromic properties.[33] Therefore, a knowledge of the photophysical and electrochemical behavior of carbazole-based compounds is necessary prior to select the suitable derivatives for the synthesis of new photosensitive polymers, optical devices or selective photosensors.

In this work, we describe the synthesis procedure and the photophysical, electrochemical and spectroelectrochemical characterization of three *N*-phenyl carbazole derivatives (Scheme 1), whose properties make them promising candidates as fluorescent probes and charge carriers. Complementary electron paramagnetic resonance spectroscopy (EPR) and DFT/TD-DFT molecular calculations were also carried out to help the interpretation of the experimental data.

ACCEPTED MANUSCRIPT

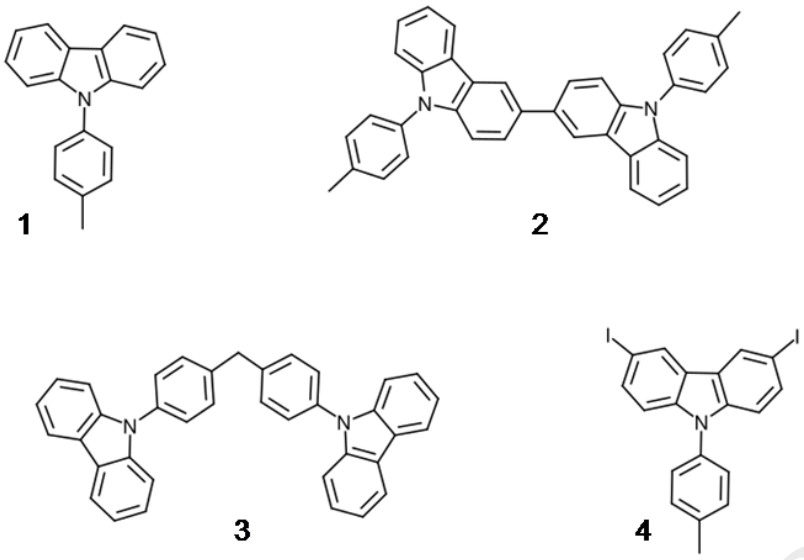

Scheme 1. Molecular structures of the *N*-(4-methyl-phenyl)-carbazole derivatives studied in this paper: **1) TCz**, **2) TCz-TCz**, **3) CzPh-CH_2-PhCz**, and **4) 3,6-ICz**. ~~(see the corresponding names in the text).~~

2. Materials and methods

2.1. Synthesis and characterization of carbazoles

All commercially available reagents used throughout this work were purchased from Aldrich and used without further purification unless otherwise stated. When necessary, reagents and solvents were purified according to standard procedures. The structures of the compounds were assigned by means of nuclear magnetic resonance (NMR) and mass spectrometry**.** The ^{1}H and ^{13}CNMR spectra were recorded on Bruker Avance-300 spectrometer with TMS as the internal standard and deuterated chloroform as solvent (Abbreviations: s = singlet, d = doublet, t = triplet, and m = multiplet, expected but not resolved). Mass spectra were performed by direct injection on a Shimadzu GCMS-QP2100ULTRA-AOC20i CGL-MS spectrometer. The atom numbering for NMR characterization is provided in Supplementary Material Information (SP01 and SP02 files).

Compound 1 [9-(4-methyl-phenyl)carbazole]: In a glass tube, 10 mL of dry toluene were mixed with 4-iodotoluene (5.25 g, 24 mmol), carbazole (4.0 g, 24 mmol), CuI (0.040 g, 0.2 mmol), 1,10-phenanthroline (0.041 g, 0.2 mmol) and potassium *tert*-butoxide (3.5 g, 31 mmol). The container was sealed and heated to 120 °C for 24 h under argon atmosphere with vigorous stirring. Then, 10 mL of toluene was added, the mixture was filtered and the solid was washed with three aliquots of 10 mL of toluene. Combined organic washings were concentrated under reduced pressure. Crude solid product was

ACCEPTED MANUSCRIPT

purified by column chromatography (silica gel, hexane/ethyl acetate 9:1). Yield: 85%. m/z= 257.12. ^{1}HNMR (300 MHz, $CDCl_3$): δ 2.49 (s, 3H, CH_3), 7.25 – 7.32 (m, 2H, H-3, H-6), 7.35 – 7.48 (m, 8H, H-1, H-8, H-2, H-7, H-2', H-3'), 8.15 (d, 2H, *J* 7.7 Hz, H-4, H-5). ^{13}CNMR (75 MHz, $CDCl_3$): δ 21.25 (CH_3), 109.78 (C-1, C-8), 119.71 (C-3, C-6), 120.25 (C-4, C-5), 123.24 (Cq-C-4, Cq-C5), 125.84 (C-2, C-7), 127.01 (C-3'), 130.47 (C-2'), 135.01 (C-4'), 137.37 (C-1'), 141.07 (Cq-C-1, Cq-C-8).

Compound 2 [9, 9'-bis(4-methyl-phenyl)-9*H*, 9'*H*-3, 3'-bicarbazole]: 9-(4-methyl-phenyl)carbazole (compound **1**; 0.27 g, 1.0 mmol) was dissolved in dichloromethane (10 mL). Anhydrous $FeCl_3$ (0.650 g, 4.0 mmol) was added and the resulting mixture turned dark green color. The reaction mixture was stirred for 6 h at room temperature. Thin layer chromatography (TLC) was used to monitor the reaction. After the reaction was completed, the solution mixture was poured in methanol. A pale-yellow precipitate was obtained, filtered and washed with methanol. The obtained pale-yellow crystals were dried and crystallized from tetrahydrofuran. Yield: 98%. m/z=512.2. ^{1}HNMR (300 MHz, $CDCl_3$): δ 2.51 (s, 6H, CH_3), 7.27 – 7.34 (m, 2H, H-2), 7.40 – 7.45 (m, 8H, H-2', H-1, H-H-3), 7.48 (d, 2H, *J* 8.5 Hz, H-8), 7.50 (d, 4H, *J* 8.5 Hz, H-3'), 7.77 (dd, 2H, *J* 8.5, *J* 1.6 Hz, H-7), 8.24 (d, 2H, *J* 7.7 Hz, H-4), 8.45 (d, 2H, *J* 1.6 Hz, H-5). ^{13}CNMR (75 MHz, $CDCl_3$): δ 21.27 (CH_3), 109.91 (C-1), 110.03 (C-8), 118.86 (C-5), 119.80 (C-2), 120.39 (C-4), 123.48 (Cq-C-1), 123.86 (C-6), 125.78 (C-7), 125.94 (C-3), 126.95 (C-3'), 130.51 (C-2'), 134.26 (Cq-C-5), 135.09 (C-4'), 137.37 (C-1'), 140.20 (Cq-C-8), 141.53 (Cq-C-4).

Compound 3 [bis(4-(9*H*-carbazol-9-yl)phenyl)methane]: In a hermetically sealed glass container, 15 mL of dry toluene were mixed with carbazole (4.0 g, 24 mmol), 4,4´–diamino-diphenyl-methane (2.4 g, 12 mmol), CuI (0.080 g, 0.4 mmol), 1,10- phenanthroline (0.081 g, 4.0 mmol) and potassium *tert*-butoxide (4.0 g, 36 mmol). The mixture was heated at 120 °C for 24 h with stirring. Then, 10 mL of toluene was added, the mixture was filtered and the solids were washed with three aliquots of 10 mL of toluene. Combined organic washings were concentrated under reduced pressure. The obtained crude solid was purified by column chromatography (silica gel, hexane/ethyl acetate 5:1) Yield: 75%. m/z=498.2. ^{1}HNMR (300 MHz, $CDCl_3$): δ 4.24 (s, 2H, CH_2), 8.16 (ddd, 4H, *J* 8.0 *J* 1.9 Hz, H-3, H-6), 7.41 (dd, 4H, *J* 8.2 *J* 1.0 Hz, H-2, H-7), 7.45 (d, 4H, *J* 8.2 Hz, H-1, H-8), 7.52 (d, 4H, *J* 8.5 Hz, H-2'), 7.56 (d, 4H, *J* 8.9 Hz, H-3'). ^{13}CNMR (75 MHz, $CDCl_3$): δ 41.34 (CH_2), 109.81 (C-1, C-8), 119.89 (C-3, C-6), 120.32 (C-4, C-5), 123.35 (Cq-C-4, Cq-C-5), 125.91

ACCEPTED MANUSCRIPT

(C-2, C-7), 127.29 (C-3'), 130.41 (C-2'), 135.96 (C-4'), 139.97 (C-1'), 140.94 (Cq-C-1, Cq-C-8).

Compound 4 [9-(4-methyl-phenyl)-3,6-diiodo-carbazole]: A mixture of 9-(4-methyl-phenyl)carbazole (5.0 g, 20 mmol), KI (7.3 g, 44 mmol), and KIO_3 (4.7 g, 22 mmol) in glacial acetic acid (200 mL) was heated at 110 °C for 6 h. The mixture was cooled and the formed precipitate was collected by suction filtration. The crude product was thoroughly washed with water and the solid was dissolved in CH_2Cl_2 (200 mL) and washed with aqueous $NaHCO_3$, dried with anhydrous Na_2SO_4 and filtered. After solvent evaporation, the pure compound was obtained by recrystallization from a mixture of CH_2Cl_2/MeOH as a white solid. Yield: 95%. m/z=509.

2.2. Spectroscopic measurements

Absorption spectra were recorded on a Hewlett Packard 8453E diode array spectrophotometer. Fluorescence measurements were carried out with a Horiba Jobin Yvon FluoroMax®-4P spectrofluorometer. The samples were analyzed on dichloromethane solutions and a 1-cm-pathlength quartz cuvette was used in all spectroscopic assays. All samples were adjusted to absorbance <0.1 at excitation wavelength (330 nm) for recording the fluorescence spectra. Solutions of quinine sulphate in H_2SO_4 0.5 mol L^{-1} were used as a recommended standard for fluorescence quantum yields determination.[34] The absorbances of standard and sample were matched at the same excitation wavelength, and were ≤0.05. Quantum yield was calculated according to Equation 1:[34]

$$\Phi_F^i = \frac{F^i A^s n_i^2}{F^s A^i n_s^2} \Phi_F^s \qquad \text{(Eq. 1)}$$

where Φ_F^i and Φ_F^s are the fluorescence quantum yield of the sample and that of the standard, respectively. F^i and F^s are the integrated intensities (areas) of sample and standard fluorescence spectra, respectively; A is the absorbed light at the excitation wavelength; n_i and n_s are the refractive index of the sample and reference solution, respectively. Both the sample and the standard where excited at the same wavelength, avoiding the introduction of an uncertainty in the relative photon flux. To minimize errors,

ACCEPTED MANUSCRIPT

we use the same sample cell and the same absorbance at the excitation wavelength for sample and reference.

Phosphorescence experiments were performed in the aforementioned FluoroMax®-4P spectrofluorometer, equipped with a phosphorimeter. A xenon flash lamp was used as irradiation source and the emitted phosphorescence was measured using an R928P photon-counting detector. Ethanolic solutions of the samples were analyzed at 77K.

The UV-Vis-NIR spectra for radical cation species were taken using a Shimadzu PC 3101 spectrometer. The EPR spectra were measured in a Bruker EPR-ELEXSYS E500, and simulated trace was calculated with Winsim 2002. Spectra of desired species were checked spectrophotometrically before EPR measurements and the solutions were degassed and sealed into capillary tubes.

2.3. Electrochemical characterization

All electrochemical experiments were recorded with a TEQ-3 potentiostat. Electrolysis and cyclic voltammetries were performed in a conventional three-electrodes electrochemical cell. Acetonitrile (HPLC grade) was used as electrolysis solvent and $TBAPF_6$ 0.1 mol L^{-1} as supporting electrolyte after the crystallization from hot ethanol. The working electrode was either indium-doped tin oxide covered glasses (ITO glasses, VisionTeK Systems, Ltd., UK) or a 0.05 mm diameter platinum disc (99.99% purity). A plate of pure gold was used as counterelectrode, and an Ag 99% purity wire was used as pseudoreference electrode. The platinum electrode was polished with 1% alumina powder in water over a piece of cloth, cleaned in an ultrasonic bath with absolute ethanol and dried in air. All redox potentials were standardized using ferrocene/ferrocenium$^+$ couple in acetonitrile and referred to NHE.[35]

Bulk electrolysis was done in home-made cell composed by two small separate compartments built with pipette tips. Two pieces of graphite felt were used as working and counterelectrodes, and a silver wire as pseudoreference electrode.

The electropolymerization was performed on ITO covered glasses of 1 cm wide immersed in a 0.01 mol L^{-1} sample solution, in electrolysis solvent and $TBAPF_6$. A constant potential of 2000 mV was applied for 15 min and then reduced to 0 mV until the current dropped to less than 1% of the initial value. The electrode was washed several times with acetonitrile. After electropolymerization, the ITO glass was placed in a 3-mL glass cuvette

ACCEPTED MANUSCRIPT

with acetonitrile and $TBAPF_6$ 0.1 mol L^{-1}. The cuvette contained a polytetrafluoro-ethylene (Teflon®) holder inside with Pt and Ag wires to be used as counter- and reference electrodes, respectively.

Spectroelectrochemistry experiments were performed in solution with a three-electrodes quartz thin layer cell using a graphite felt as counterelectrode, platinum woven wire as working electrode (70 μm wires), and a silver pseudoreference electrode. Absorption spectra were measured in the aforementioned Shimadzu UV-3101PC spectrophotometer.

2.4. Computational Methods

Density functional theory (DFT) calculations with the Coulomb attenuated CAM-B3LYP exchange-correlation functional and a split valence 6-31G+* basis set were performed to obtain the optimized ground state geometry.[36] SCRF model IEFPCM was used for simulating the solvation effects.[37-40] Vibrational frequency calculations were carried out to characterize the stationary points and no imaginary frequencies were found. Excited state energies and optimized geometries were calculated with linear response time-dependent density functional theory (TD-DFT). All calculations were performed with Gaussian 09,[41] and Gabedit[42] was used to visualize molecular orbitals (MOs). The VMD 1.8.9 program was used for graphics rendering.[43] Supplementary material SP03 shows output coordinates of DFT calculations.

3. Results and discussion

3.1. Synthesis of carbazoles and photophysical properties

The molecular structures of the *N*-(4-methyl-phenyl) carbazole derivatives synthesized are depicted in Scheme 1. In order to highlight their distinctive structural features, from now on the molecules will be renamed as follows: **1) TCz** (*N*-tolyl-carbazol); **2) TCz-TCz** (3,3´-dimer); **3) CzPh-CH_2-PhCz** (methylene-bridged *N*-phenyl-carbazole); and **4) 3,6-ICz** (3,6-iodide-carbazole). **TCz-TCz** was synthesized according to the procedure described by Zhang *et al.* for analog derivatives,[44] yielding a very high percentage of desired product (at around 100%). On the other hand, reported synthetic pathways for **TCz** and **CzPh-CH_2-PhCz**[45, 46] were modified in order to apply milder reaction conditions that improve yields. This optimization was based on the work of Kelkar

ACCEPTED MANUSCRIPT

et al.[47] who developed a single-step catalytic synthesis of arylamines by using chelating ligands, which enhanced the product yields significantly. In Scheme 2 are depicted the synthesis of **CzPh-CH$_2$-PhCz** performed with a combination of 1,10-phenantroline (Phen) and CuI as ligand/catalyst complex, in the presence of potassium *tert*-butoxide base (K^+t-but$^-$). A yield at around 75% was obtained, a value over 3-fold greater than the 23% previously reported by He *et al.*[46]

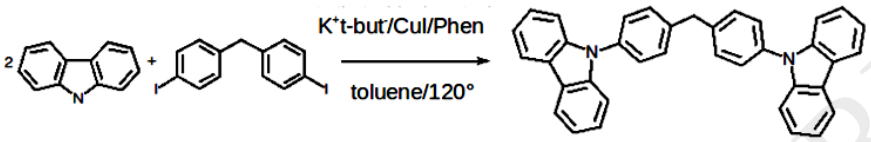

Scheme 2. Optimized procedure for the synthesis of **CzPh-CH$_2$-PhCz** (see Materials and methods section for details)

The ground and singlet excited states of synthesized carbazole derivatives were characterized in dichloromethane solutions by means of absorption and fluorescence spectra (Figure 1). For the sake of comparison, some spectra were also recorded in absolute ethanol. In Table 1 are summarized the photophysical parameters obtained along with reported data for some related compounds.

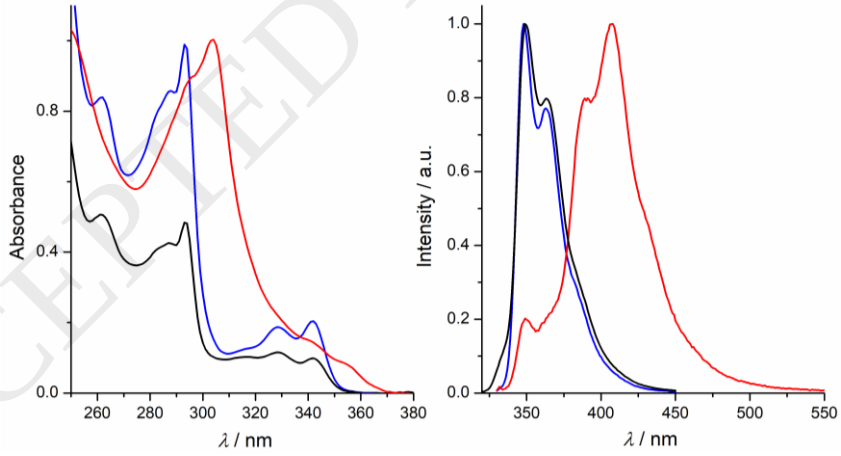

Figure 1. Absorption (left, ordinates as shown) and fluorescence (right, ordinates normalized) spectra of the compounds **TCz**, (black), **TCz-TCz** (red) and **CzPh-CH$_2$-PhCz** (blue) in CH_2Cl_2 solution. The emission spectra were recorded by exciting the samples at 330 nm.

Figure 1 shows that the studied compounds registered absorption in the UV region with two main bands at around 290-300 and 330-350 nm, typical of carbazole moiety.[10] In the case of **TCz** and **CzPh-CH$_2$-PhCz** almost identical absorption and fluorescence

ACCEPTED MANUSCRIPT

spectra were recorded, and the data obtained for **CzPh-CH$_2$-PhCz** are in agreement with those previously reported.[46] Also, the UV absorption spectrum of **TCz-TCz** in Figure 1 resembles that of the *N*-phenyl-carbazole dimer linked at 3, 3´positions, recently reported by Tang *et al*.[30] As it can be seen on Table 1, only slight differences were observed in the spectra recorded in ethanol with respect to those measured in CH_2Cl_2. In spite of the electron lone pairs on the nitrogen atoms, these results suggest that no specific interactions (such as hydrogen bonds) are occurring between carbazoles and the protic solvent. Similar results were reported by other authors with several *N*-substituted carbazoles in polar and non-polar solvents (see Table 1 for some examples).[10, 48]

Table 1. Summary of spectroscopic properties of carbazoles derivatives in CH_2Cl_2 solution (some data in ethanol are denoted with "‡").

	Compound	λ_{abs} / nm	λ_{em} / nm	$\Delta\nu$ / cm^{-1}	Φ_F[a]
1	Cz[b]	292, 334	338, 354	354	0.37
2	MeCz[b]	296, 346 294, 344‡	351, 365 350, 363‡	412 498‡	0.26 0.32‡
3	PhCz	294, 340[b] 292, 340‡[b] 292, 326, 339‡[c]	346, 359[b] 347, 360‡[b] 345, 359‡[c]	510 593 513	0.28[b] 0.31‡[b]
4	**TCz**	293, 329, 342	348, 363	504	0.34
5	**CzPh-CH$_2$-PhCz**	293, 329, 342 293, 328, 341[d]	349, 363 350, 365[d]	586 754	0.31 0.21[d]
6	**TCz-TCz**	304, 342, 356 303, 341, 355‡	390, 407 385, 403‡	2449 2195	0.12
7	EtCz-EtCz[e]	358	414	3543	-
8	Biphenyl[f]	248	305, 315	7536	0.18
9	TMB[g]	310	401	7320	0.13
10	TPB[h]	349	400	3653	0.73

a) Relative to quinine sulphate in H_2SO_4 0.5 mol L^{-1}. Estimated error ±10%.

b) Non-substituted carbazole (Cz), *N*-methyl-carbazole (MeCz), and *N*-phenyl carbazole (PhCz), Ref. [10]

c) Estimated from spectra of PhCz, Ref. [48]

d) Ref. [46]

e) Dimer of *N*-ethyl carbazole linked at 3, 3´positions in toluene, Ref. [49]

f) Ref. [50]

g) *N,N,N′,N′*-Tetramethyl-benzidine, Ref. [51]

h) *N,N,N′,N′*-Tetraphenyl-benzidine, Ref. [52]

ACCEPTED MANUSCRIPT

A close examination on Table 1 reveals that the spectroscopic features of carbazoles seem to be independent on the substitution at the *N* position. This becomes evident if the entries 2-5 are compared to each other (idem by comparing the dicarbazoles 6-7 to each other). Such results can be explained by analyzing the MOs involved in the electronic transitions that give rise to the absorption and emission spectra. Figure 2 depicts the optimized geometries and the highest occupied molecular orbitals (HOMOs) corresponding to the ground and singlet excited state of **TCz**. It can be seen that both HOMOs are localized on the carbazole planar rings, with the *N*-phenyl moiety twisted out of the planarity and electronically uncoupled with the rest of the molecule. Therefore, such twisted configuration is responsible for the spectral properties being insensitive to the presence of either an alkyl- or phenyl- substituent at *N* position.

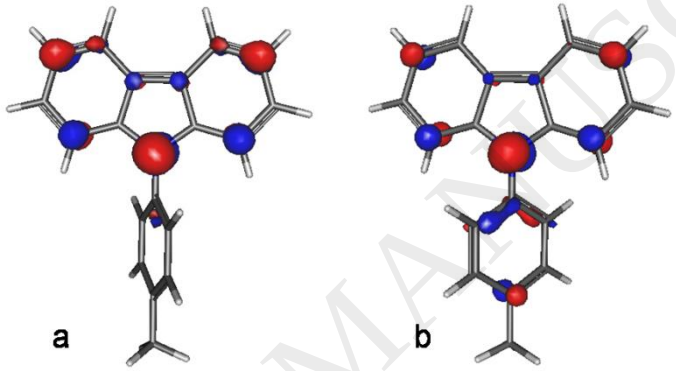

Figure 2. Optimized geometries and HOMOs for ground a) and singlet excited state b) of **TCz**.

Furthermore, although the twisted configuration of the *N*-phenyl moiety is also present in both carbazole fragments of **CzPh-CH$_2$-PhCz** and **TCz-TCz** (Figure 3), the spectroscopic behavior is very different when the linkage is on the planar rings of carbazole structure. For **TCz-TCz**, average red shifts of 13 nm in absorption and 43 nm in fluorescence bands with respect to those of **TCz** (and **CzPh-CH$_2$-PhCz**) is a clear sign of increased conjugation. From Table 1, similar red shifts can be calculated (12 nm in absorption and 49 nm in fluorescence bands) by analyzing the reported results for **EtCz-EtCz**,[49] with respect to single **MeCz**[10] in non-polar solvents. Differences in conjugation between **CzPh-CH$_2$-PhCz** and **TCz-TCz** are apparent in Figure 3, where HOMOs are compared for both molecules. Note that localization of the HOMO in the ground state of both dicarbazoles is on their planar π-system (see Figure 3a-b), although conjugation only extends when fragments are bound at 3,3' position (**TCz-TCz**) and not when the linkage is by methylene-bridged *N*-phenyl substituents (**CzPh-CH$_2$-PhCz**). Singlet excited states

ACCEPTED MANUSCRIPT

follow the same behavior. Moreover, although free rotation around methylene bridge is possible for **CzPh-CH$_2$-PhCz**, we have not found any orientation that promotes (through space) an extension of the delocalized π-system between both phenyl (close) or planar rings (far) by orbital coupling. This observation suggests that not only *N*-phenyl- twisting but also the methylene bridge disrupt any molecular orbital coupling between both **TCz** fragments and therefore, they behave as two isolated chromophores. For these reasons, the spectral features of **CzPh-CH$_2$-PhCz** match those of single **TCz**.

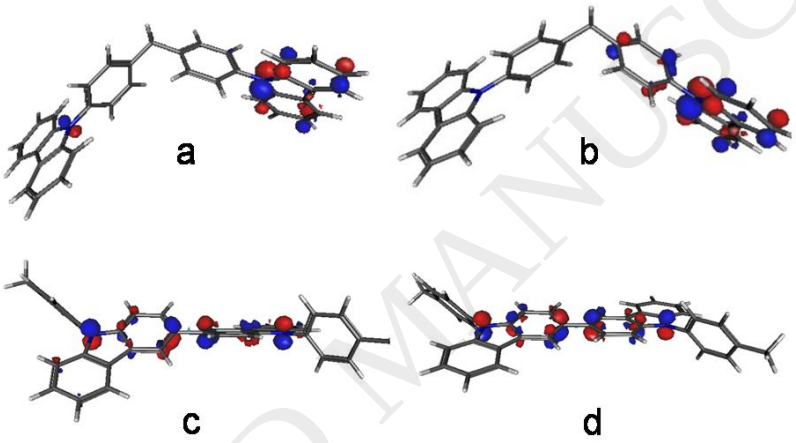

Figure 3. Optimized geometries and HOMOs for: **TCz-TCz** in the ground a) and singlet excited state b); and **CzPh-CH$_2$-PhCz** in the ground c) and singlet excited state d).

Stokes shifts (energy gap between the longest wavelength absorption band and the shortest emission one, $\Delta\nu$) are also shown in Table 1. It is clear that dicarbazoles bound at 3,3' position (entries **6-7**) experience larger Stokes shifts than the others (entries **1-5**), diagnostic of difference in equilibrium geometry between ground and singlet excited states. Optimized geometries for both states in **TCz-TCz** and **CzPh-CH$_2$-PhCz** are also shown in Figure 3. Dihedral angle in **TCz-TCz** involving the 3,3´ bond shifts from 40 degrees in the ground state to 12 degrees in the excited state, imposing near-coplanarity between the adjacent carbazoles. This geometric rearrangement gives rise to the larger Stokes shift of **TCz-TCz** and **EtCz-EtCz** compared to the emission from single carbazole rings.

ACCEPTED MANUSCRIPT

Last column in Table 1 shows the fluorescence quantum yields (Φ_F) of analyzed and some related compounds. As it can be seen, the data tend to two clearly different Φ_F values. Firstly, Φ_F values at around 0.30 were obtained for **TCz** and **CzPh-CH$_2$-PhCz** and agree with those reported for compounds with only one carbazole fragment (see entries **1-5**). As described above, the two carbazoles of **CzPh-CH$_2$-PhCz** are electronically uncoupled and, therefore, its Φ_F is analogous to those of single carbazole compounds. On the other hand, a lower Φ_F value (less than half of the previous ones) was obtained for **TCz-TCz**. A close examination of Figure 3 reveals that the HOMOs in **TCz-TCz** expand over a portion of the molecule that resembles a biphenyl-like or even a benzidine-like structure. Table 1 shows that the Φ_F values for **TCz-TCz**, biphenyl and *N,N,N′,N′*-tetramethyl-benzidine are very similar, which suggests that the extra molecular rigidity promoted by the π-system extended favors the radiationless deactivation pathways. Note the contrast with *N,N,N′,N′*-tetraphenyl-benzidine (Table 1), which shows that fluorescence deactivation is the preferred way when free-rotating arylamines are part of the biphenyl-like skeleton. Therefore, the decreasing in Φ_F of **TCz-TCz** compared with electronically-single carbazoles might be ascribed to an increase in the intersystem crossing quantum yield, and not just to internal energy conversion from the singlet excited state to surrounding solvent. This possible trend to triplet states formation is a relevant and suitable characteristic for the application of this type of compounds as phosphorescent-sensitizers in electroluminescence. To obtain some insights about this, phosphorescence spectrum of **TCz-TCz** in solvent glass at 77K was recorded by exciting the sample at 330 nm (Figure 4). From the triplet emission maximum (476 nm) a S_0-T_1 energy gap of 2.61 eV can be calculated for **TCz-TCz**, which is comparable to those reported for 3,3´-linked dicarbazoles,[49, 53] and is near the limit value for a suitable host in blue electroluminescent materials. Finally, although smaller than arylamines, the values of Φ_F obtained for these carbazoles make them still appropriate to develop selective probes in fluorescence sensing.

ACCEPTED MANUSCRIPT

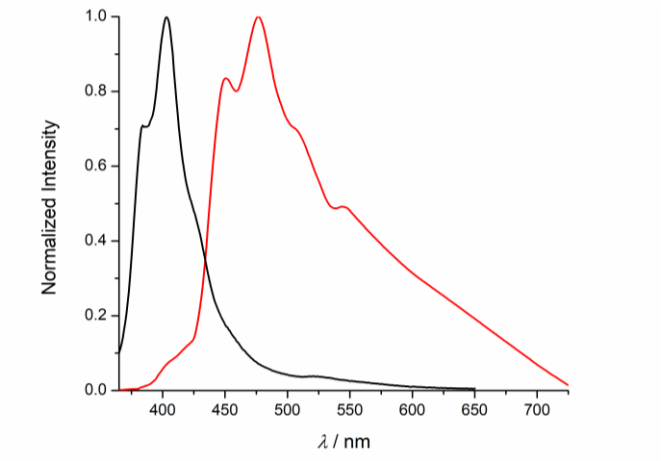

Figure 4. Normalized emission spectra of **TCz-TCz** in ethanol: fluorescence (black) in solution at 298K, and phosphorescence (red) in solvent glass at 77K.

3.2. Electrochemical and spectroelectrochemical characterization

Figure 5 shows the absorption spectra of **TCz-TCz** recorded spectroelectrochemically. The cyclic voltammetry of **TCz-TCz** (inset in Figure 5) showed two reversible waves at 1280 y 1575 mV (vs. NHE) corresponding to the oxidation of the nitrogen atoms in each carbazole fragment. At increasing potential, two simultaneous absorption bands (one at 417 nm and a complex broad at 917 nm) are observed, which are associated to the first oxidation potential. The near-infrared absorption band (917 nm) can be ascribed to a mixed valence charge transfer, so the first monoxidized specie, **TCz-TCz$^{\bullet+}$**, would be a mixed valence ion.

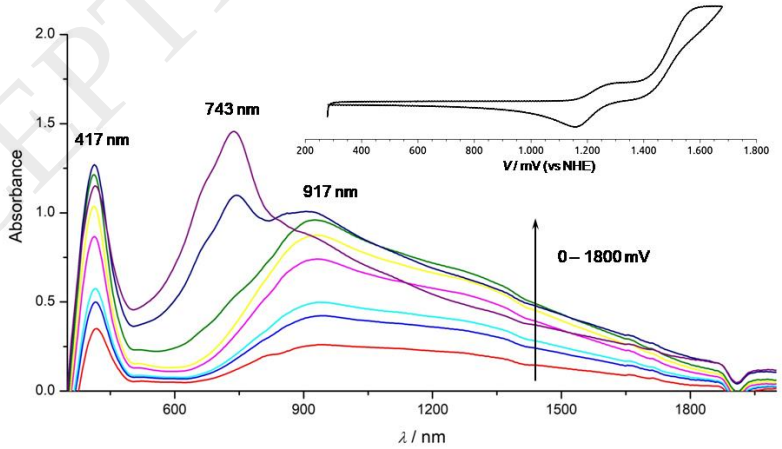

Figure 5. Absorption spectra of **TCz-TCz** in Cl_2CH_2 obtained by spectroelectrochemistry from 0 to 1800 mV vs. NHE. Inset: cyclic voltammetry in Cl_2CH_2 with $TBAPF_6$ 0.1 mol L^{-1}.

In order to understand the electronic density distribution of this radical cation (either localized or delocalized in both carbazole fragments), we performed the ESR spectrum of ex-situ

ACCEPTED MANUSCRIPT

electrogenerated **TCz-TCz$^{\bullet+}$**. The correlation between the theoretical simulated spectrum and the experiment was 99.8% (Figure 6). Table 2 shows the hyperfine coupling constants fitted, considering all nitrogen and hydrogen atoms. It is remarkable that both nitrogen atoms have the same hyperfine coupling constant, a clear indication of a spin delocalized over the two redox centers on the ESR time scale. This reinforces the mixed-valence character of the radical ion **TCz-TCz$^{\bullet+}$**, and strongly suggests a Robin and Day's Class III (delocalized) classification.[54, 55]

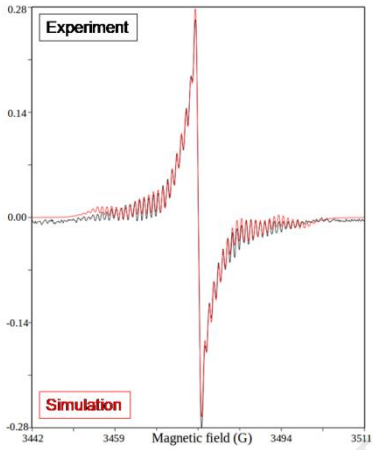

Figure 6. Black: high resolution EPR spectrum (at 298 K, width = 50 Gauss) of **TCz-TCz$^{\bullet+}$** in Cl_2CH_2 obtained by oxidation in an electrolytic cell with $TBAPF_6$ 0.1 mol L^{-1}. Red: simulated spectrum with coupling constants fitted using WINSIM 2002.

Table 2. Coupling constants found by simulation of ESR spectrum of **TCz-TCz$^{\bullet+}$**.

Atom	2N	2H	2H	4H	6H
Coupling constant/Gauss	8.77	3.06	2.90	0.95	0.90

The spin density isosurface of **TCz-TCz$^{\bullet+}$** is showed in Figure 7. It can be inferred from the spin distribution that the positive charge lies mostly on the two nitrogen and on the two sets of two hydrogen atoms each, displaying a symmetric pattern on the biphenyl part of the molecule (a delocalized hole), in agreement with the ESR experiment.

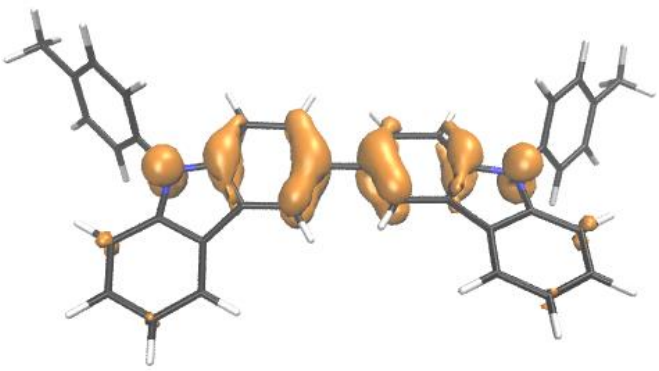

ACCEPTED MANUSCRIPT

Figure 7. CAM-B3LYP unpaired spin density (0.004 a.u.) obtained for **Tcz-Tcz$^{\bullet+}$**.

As the oxidizing potential increased another absorption band arose at 743 nm, whereas a decrease in the NIR absorption was observed (see Figure 5). This resembles the spectrum measured for oxidized **3,6-ICz$^{\bullet+}$** ~~(Figure 8, discussion below)~~ (see Figure S1 in Supplementary material), in which there is no intervalence band. This fact is associated to the complete oxidation of both carbazole fragments to form the dication **TCz-TCz^{2+}**. A similar behavior was observed in the double oxidation of tetratolyl-benzidine, having two electronically coupled triarylamine units as electroactive fragments.[56, 57]

On the other hand, **CzPh-CH$_2$-PhCz** showed a different electrochemistry. A complex process was observed in the first voltammogram (Figure 8a), with an first oxidation wave at 1510 mV and reduction waves around 1250 and 1450 mV. The different height and shape of the current peaks suggest that a coupled chemical process takes place, in which the oxidized species participates. In the successive cycles, two new reversible waves were observed at around 1300-1450 mV and 1500-1800 mV. The new shape of the voltammogram was typical of that registered when a species is adsorbed and accumulated on the electrode. In order to verify this assignment, the Pt electrode was rinsed with clean solvent to remove the soluble **CzPh-CH$_2$-PhCz** and immersed in a fresh electrolysis solution. The voltammogram of this sample showed the disappearance of the original waves at 1600 mV and the permanence of the recently formed peaks at 1110 (cat.) and 1621 (an.) mV, and 1450 (cat.) and 1917 (an.) mV (~~Figure 9b~~ Figure 8b).

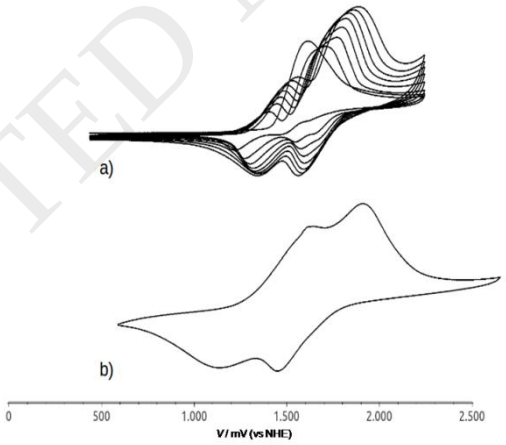

Figure 8. a) Cyclic voltammetry of **CzPh-CH$_2$-PhCz** (0.01 mol L^{-1}) in electrolysis solution. Scan rate: 25 mV s^{-1}. b) Cyclic voltammetry of electrodeposited film on ITO glass in electrolysis solution (free of **CzPh-CH$_2$-PhCz**).

In order to obtain more insights about the adsorbed species, we performed a spectroelectrochemical experiment on the film electrodeposited by oxidation using ITO as working electrode. The absorption spectrum in Figure 9 shows that two successive species arise as the

ACCEPTED MANUSCRIPT

film oxidizes with the applied potential, from 0 to 2000 mV. The first one with absorption band centered at 432 and another with a broad band at around 1400 nm, the latter being ascribed to an intervalence compound similar to **TCz-TCz** described above (bands at 417 y 917 nm in Figure 5).

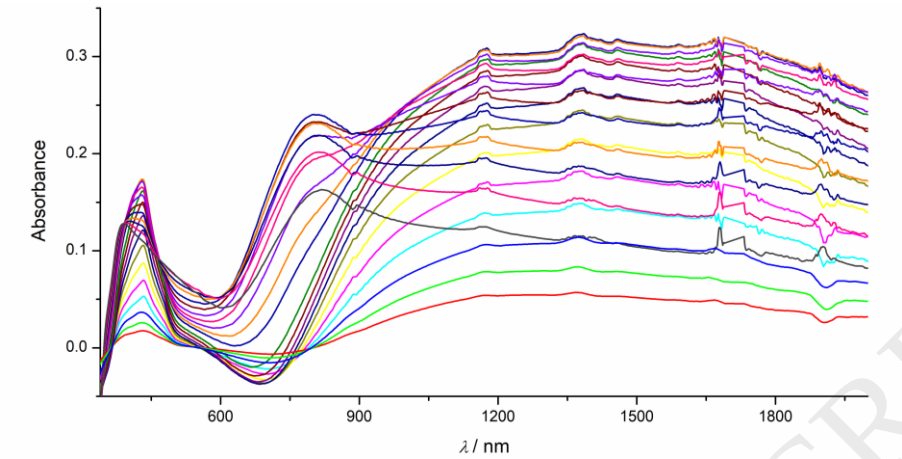

Figure 9. Absorption spectra obtained by spectroelectrochemistry of electropolimerized film deposited on ITO glass, at applied potentials from 0 to 1800 mV.

This electrochemical behavior, along with the formation of a NIR absorbing species resembles that of methylene-bridged phenylamines previously reported by our group,[58] in which phenylamine moieties form (by oxidative coupling) a benzidine fragment. It was observed that the film did not remained adsorbed on the ITO surface beyond 9 potential step cycles spanning 1000 seconds from an all-reduced to an all-oxidized state (Figure 10). This behavior is contrary to that of methylene-bridged phenylamine polymer,[58] which showed to be highly insoluble and stable. The formation of this polymer can be understood by comparison with the electrochemistry of both **TCz** and **3,6-ICz** in acetonitrile solution.

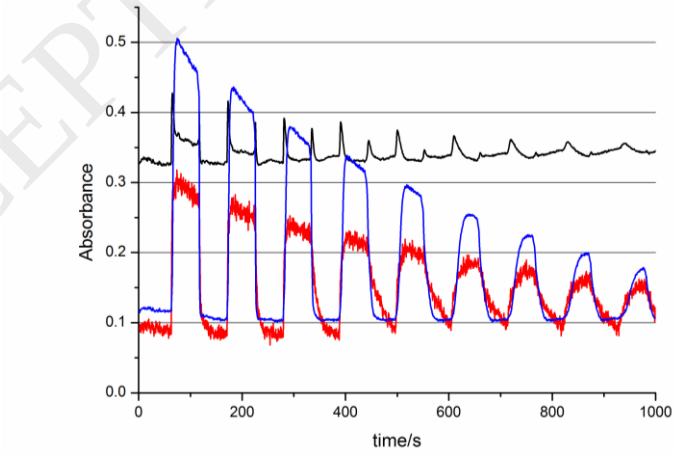

Figure 10. Absorbance of the electropolymerized film at 420 nm (red), 790 nm (black) and 900 nm (blue), from 0 to 2000 mV during 1000 seconds.

ACCEPTED MANUSCRIPT

TCz has a complex behavior showing an irreversible oxidation wave at 1500 mV and a reduction process at 1200 mV (inset in Figure 11). According to ~~Figure 12~~ Figure 11, several absorption bands were observed from the spectroelectrochemistry experiments, which can be ascribed to two different species: the first one with bands at 410 and 909 nm, and the second one with absorption at around 693 nm. Although it was not possible to isolate the species formed after the electrochemical oxidation, the sequence in spectra resembles that of **TCz-TCz$^{\bullet+}$**, so it suggests that this fragment appears during the voltammetry. Similar results were reported for analogous compounds.[59]

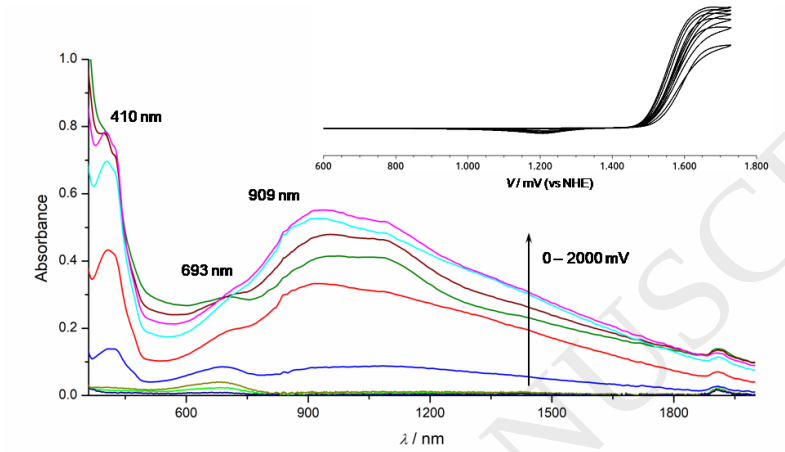

Figure 11. Absorption spectra of **TCz** in Cl_2CH_2 obtained by spectroelectrochemistry, with applied potential from 0 to 2000 mV vs. NHE. Inset: cyclic voltammetry in Cl_2CH_2 with TBAPF6 0.1 mol L^{-1}.

Since carbazole derivatives having free 3 and 6 positions are reported to form dimers when oxidized (actually, it is the way by means **TCz-TCz** was synthesized in the present work), we performed an electrochemical study of **3,6-ICz,** which is substituted with iodine at the 3 and 6 positions, so preventing any coupling. As expected (figure S1 in Supplementary material), the cyclic voltammetry of **3,6-ICz** (inset) ~~Figure 8 (inset)~~ shows a reversible wave at 1650 mV without any coupled homogeneous processes and from espectroelectrochemistry only two bands at 350 and 590 nm ascribed to the radical **3,6-ICz$^{\bullet+}$** were observed. These bands have also been recorded with other 3,6-disubstituted carbazoles, whose electronic structure were described elsewhere.[60] Moreover, no absorptions were detected in NIR, as expected for a non dimeric species.

In contrast to **TCz-TCz** (whose monooxidized cation is not further reactive for polymerization), each redox fragment in **CzPh-CH_2-PhCz** behaves as a single **TCz** forming independent **–CH_2-TCz-TCz-CH_2–** subfragments by coupling with other oxidized molecules in solution, no matter the state of the aliphatically bound (and beyond the metylene bridge) **TCz** in the same molecule. Polymerization, then, generates high amounts of electronically disconnected units, responsible for the electrochromic response, each one electronically very similar to **TCz-TCz** (see analogy between ~~Figure 10~~ Figure 9 and ~~Figure 12~~ Figure 11). As seen in the related phenylamine

ACCEPTED MANUSCRIPT

polymer,[60] the absence of delocalization between the redox centers on both ends of the methylene bridge forces electronic hopping as the main electron transport mechanism in the (now) **TCz-TCz** methylene bridged film.

4. Conclusions

Based on a combination of reported procedures, a series of *N*-(4-methylphenyl)-carbazole derivatives were synthesized and purified with high yields. Absorption and fluorescence spectra of these molecules were recorded, which showed spectroscopic features analogous to those of some related compounds previously reported. DFT and TD-DFT calculations showed that the *N*-(4-methylphenyl) ring is not electronically coupled to the rest of the system, unlike triphenylamine compounds previously studied by our group. Furthermore, by analyzing the molecular orbitals could be seen that the methylene bridge in **CzPh-CH_2-PhCz** promotes the uncoupling of the two carbazole units, whereas linkage at 3,3´-position in **TCz-TCz** extends the π-system along of both fragments.

Oxidation of **CzPh-CH_2-PhCz** yields **TCz-TCz** units separated by methylene bridges in a polymeric form that resulted in less stable film on the ITO surface than those formed by benzidine units. The near-infrared band at around 1000 nm (either in soluble **TCz-TCz** or in polymer) is assigned to the intervalence charge transfer between carbazole subunits of **TCz-TCz** fragments. It should be noted that although intervalence transitions in delocalized molecules do not transfer net charge between redox centers (it resembles a $\pi \rightarrow \pi^*$ transition), they are usually classified as “charge transfers” because are a special case of them under the same theory.

The radical cation of **TCz-TCz** is electronically delocalized, allowing that the positive charge (hole) is symmetrically distributed on the molecule. This compound (either as a single molecule or as part of the polymer) behaves as Class III in Robin and Day classification. The lower fluorescence quantum yield of **TCz-TCz** compared to single carbazoles suggests a favorable intersystem crossing to triplet state, which was found at 2.61 eV above ground state. This value suggests that the fragment //-CH_2-TCz-TCz-CH_2-// is a suitable candidate for green-blue electroluminescent host polymer material. Also, the still decent values of fluorescence quantum yields obtained shows that this family of compounds may be interesting for selective probes in fluorescence sensing.

Acknowledgments

ACCEPTED MANUSCRIPT

This paper is based on a project supported by ANPCYT (research project PICT 1439/2013). E. M. A. thanks to Universidad Nacional de Río Cuarto and CONICET for financial support. A. R. P and C. L. R. thank to Universidad Nacional de Mar del Plata for financial support and INBIOTEC-CONICET. M. I. M thanks to IQUIR - Universidad Nacional de Rosario for financial support. All authors are research staff at CONICET.

ACCEPTED MANUSCRIPT

ACCEPTED MANUSCRIPT

References

[1] Joanna O, Mateusz G, Roman P, Dariusz B. Pol J Chem Technol. 2014;16(1):75-80.
[2] He T, Gao Y, Chen R, Ma L, Rajwar D, Wang Y, et al. Multiphoton Harvesting in an Angular Carbazole-Containing Zn(II)-Coordinated Random Copolymer Mediated by Twisted Intramolecular Charge Transfer State. Macromol. 2014;47(4):1316-24.
[3] Cao P-F, Rong L-H, de Leon A, Su Z, Advincula RC. A Supramolecular Polyethylenimine-Cored Carbazole Dendritic Polymer with Dual Applications. Macromol. 2015;48(19):6801-9.
[4] Venkatesh Y, Rajesh Y, Karthik S, Chetan AC, Mandal M, Jana A, et al. Photocaging of Single and Dual (Similar or Different) Carboxylic and Amino Acids by Acetyl Carbazole and its Application as Dual Drug Delivery in Cancer Therapy. J Org Chem. 2016;81(22):11168-75.
[5] Higginbotham H, Karon K, P. L, Data P. Carbazoles in Optoelectronic Applications. Disp Imaging. 2017;2(3-4):207-16.
[6] Shin BS, Yoon CW, Kwak SK, Kang JW. Thermodynamic assessment of carbazole-based organic polycyclic compounds for hydrogen storage applications via a computational approach. Int J Hydrogen Energy. 2018;43(27):12158-67.
[7] Wang H, Sheikh AD, Feng Q, Li F, Chen Y, Yu W, et al. Facile Synthesis and High Performance of a New Carbazole-Based Hole-Transporting Material for Hybrid Perovskite Solar Cells. ACS Photonics. 2015;2(7):849-55.
[8] Wu J, Xie Y, Chen X, Deng GJ. Transition Metal-Free Carbazole Synthesis from Arylureas and Cyclohexanones. Adv Synth Catal. 2016;358(20):3206-11.
[9] Wex B, Kaafarani BR. Perspective on carbazole-based organic compounds as emitters and hosts in TADF applications. J Mater Chem C. 2017;5(34):8622-53.
[10] Bonesi SM, Erra-Balsells R. Electronic spectroscopy of carbazole and N- and C-substituted carbazoles in homogeneous media and in solid matrix. J Lumin. 2001;93(1):51-74.
[11] Bonesi SM, Erra-Balsells R. Electronic spectroscopy of N- and C-substituted chlorocarbazoles in homogeneous media and in solid matrix. J Lumin. 2002;97(2):83-101.
[12] Ponce María B, Cabrerizo Franco M, Bonesi Sergio M, Erra-Balsells R. Synthesis and Electronic Spectroscopy of Bromocarbazoles. Direct Bromination of N- and C-Substituted Carbazoles by N-Bromosuccinimide or a N-Bromosuccinimide/Silica Gel System. Helv Chim Acta. 2006;89(6):1123-39.
[13] Bonesi SM, Mesaros M, Cabrerizo FM, Ponce MA, Bilmes GM, Erra-Balsells R. The photophysics of nitrocarbazoles used as UV-MALDI matrices: Comparative spectroscopic and optoacoustic studies of mononitro- and dinitrocarbazoles. Chem Phys Lett. 2007;446(1):49-55.
[14] Kato S-i, Yamada Y, Hiyoshi H, Umezu K, Nakamura Y. Series of Carbazole–Pyrimidine Conjugates: Syntheses and Electronic, Photophysical, and Electrochemical Properties. J Org Chem. 2015;80(18):9076-90.
[15] Damit EF, Nordin N, Ariffin A, Sulaiman K. Synthesis of Novel Derivatives of Carbazole-Thiophene, Their Electronic Properties, and Computational Studies. J Chem. 2016;2016:14.
[16] You J, Shan Y, Zhen L, Zhang L, Zhang Y. Determination of peptides and amino acids from wool and beer with sensitive fluorescent reagent 2-(9-carbazole)-ethyl chloroformate by reverse phase high-performance liquid chromotography and liquid chromotography mass spectrometry. Anal Biochem. 2003;313(1):17-27.
[17] Shao J, Lin H, Lin H. Rational design of a colorimetric and ratiometric fluorescent chemosensor based on intramolecular charge transfer (ICT). Talanta. 2008;77(1):273-7.
[18] Yang L, Zhu W, Fang M, Zhang Q, Li C. A new carbazole-based Schiff-base as fluorescent chemosensor for selective detection of Fe3+ and Cu2+. Spectrochim Acta Part A: Mol Biomol Spectrosc. 2013;109:186-92.
[19] Gupta VD, Padalkar VS, Phatangare KR, Patil VS, Umape PG, Sekar N. The synthesis and photo-physical properties of extended styryl fluorescent derivatives of N-ethyl carbazole. Dyes Pigments. 2011;88(3):378-84.
[20] Konidena RK, Thomas KRJ, Kumar S, Wang Y-C, Li C-J, Jou J-H. Phenothiazine Decorated Carbazoles: Effect of Substitution Pattern on the Optical and Electroluminescent Characteristics. J Org Chem. 2015;80(11):5812-23.

ACCEPTED MANUSCRIPT

[21] Gawale Y, Adarsh N, Kalva Sandeep K, Joseph J, Pramanik M, Ramaiah D, et al. Carbazole-Linked Near-Infrared Aza-BODIPY Dyes as Triplet Sensitizers and Photoacoustic Contrast Agents for Deep-Tissue Imaging. Chem – Eur J. 2017;23(27):6570-8.
[22] Yilmaz G, Tuzun A, Yagci Y. Thioxanthone–carbazole as a visible light photoinitiator for free radical polymerization. J Polym Sci, Part A: Polym Chem. 2010;48(22):5120-5.
[23] Al Mousawi A, Garra P, Dumur F, Bui T-T, Goubard F, Toufaily J, et al. Novel Carbazole Skeleton-Based Photoinitiators for LED Polymerization and LED Projector 3D Printing. Mol. 2017;22(12).
[24] Al Mousawi A, Arar A, Ibrahim-Ouali M, Duval S, Dumur F, Garra P, et al. Carbazole-based compounds as photoinitiators for free radical and cationic polymerization upon near visible light illumination. Photochem Photobiol Sci. 2018;17(5):578-85.
[25] Lv H-j, Zhang X-t, Wang S, Xing G-w. Assembly of BODIPY-carbazole dyes with liposomes to fabricate fluorescent nanoparticles for lysosomal bioimaging in living cells. Analyst. 2017;142(4):603-7.
[26] Grazulevicius JV, Strohriegl P, Pielichowski J, Pielichowski K. Carbazole-containing polymers: synthesis, properties and applications. Prog Polym Sci. 2003;28(9):1297-353.
[27] K. N, H. M. Novel Complex Polymers with Carbazole Functionality by Controlled Radical Polymerization. Int J Polym Sci. 2012;2012(ID 170912).
[28] Ates M, Uludag N. Carbazole derivative synthesis and their electropolymerization. J Solid State Electrochem. 2016;20(10):2599-612.
[29] Bagnich SA, Rudnick A, Schroegel P, Strohriegl P, Köhler A. Triplet energies and excimer formation in *meta*- and *para*-linked carbazolebiphenyl matrix materials. Phil Trans R Soc A. 2015;373:20140446.
[30] Tang G-M, Chi R-H, Wan W-Z, Chen Z-Q, Yan T-X, Dong Y-P, et al. Tunable photoluminescent materials based on two phenylcarbazole-based dimers through the substituent groups. J Lumin. 2017;185:1-9.
[31] Chen JP, Natansohn A. Synthesis and Characterization of Novel Carbazole-Containing Soluble Polyimides. Macromol. 1999;32(10):3171-7.
[32] H. L, Y. Z, Y. H, D. M, L. W, X. J, et al. Novel Soluble N-Phenyl-Carbazole-Containing PPVs for Light-Emitting Devices: Synthesis, Electrochemical, Optical, and Electroluminescent Properties. Macromol Chem Phys. 2004;205(2):247-55.
[33] Hsiao S-H, Lin S-W. Electrochemical synthesis of electrochromic polycarbazole films from N-phenyl-3,6-bis(N-carbazolyl)carbazoles. Polym Chem. 2016;7(1):198-211.
[34] Brouwer AM. Standards for photoluminescence quantum yield measurements in solution (IUPAC Technical Report). Pure Appl Chem. 2011;83(12):2213-28.
[35] Noviandri I, Brown KN, Fleming DS, Gulyas PT, Lay PA, Masters AF, et al. The Decamethylferrocenium/Decamethylferrocene Redox Couple: A Superior Redox Standard to the Ferrocenium/Ferrocene Redox Couple for Studying Solvent Effects on the Thermodynamics of Electron Transfer. J Phys Chem B. 1999;103(32):6713-22.
[36] Yanai T, Tew DP, Handy NC. A new hybrid exchange–correlation functional using the Coulomb-attenuating method (CAM-B3LYP). Chem Phys Lett. 2004;393(1):51-7.
[37] Mennucci B, Tomasi J. Continuum solvation models: A new approach to the problem of solute's charge distribution and cavity boundaries. J Chem Phys. 1997;106(12):5151-8.
[38] Mennucci B, Cancès E, Tomasi J. Evaluation of Solvent Effects in Isotropic and Anisotropic Dielectrics and in Ionic Solutions with a Unified Integral Equation Method: Theoretical Bases, Computational Implementation, and Numerical Applications. J Phys Chem B. 1997;101(49):10506-17.
[39] Tomasi J, Mennucci B, Cancès E. The IEF version of the PCM solvation method: an overview of a new method addressed to study molecular solutes at the QM ab initio level. J Mol Struct: THEOCHEM. 1999;464(1):211-26.
[40] Chipman DM. Reaction field treatment of charge penetration. J Chem Phys. 2000;112(13):5558-65.
[41] Frisch MJ, Trucks GW, Schlegel HB, Scuseria GE, Robb MA, Cheeseman JR, et al. Gaussian 09W, Revision A. 1. Wallingford (CT): Gaussian. Inc; 2009.
[42] Allouche A-R. Gabedit—A graphical user interface for computational chemistry softwares. J Comput Chem. 2010;32(1):174-82.
[43] Humphrey W, Dalke A, Schulten K. VMD: Visual molecular dynamics. J Mol Graph. 1996;14(1):33-8.
[44] Zhang Q, Zhuang H, He J, Xia S, Li H, Li N, et al. Improved ternary memory performance of donor-acceptor structured molecules through cyano substitution. J Mater Chem C. 2015;3(26):6778-85.

ACCEPTED MANUSCRIPT

[45] Kim SH, Cho I, Sim MK, Park S, Park SY. Highly efficient deep-blue emitting organic light emitting diode based on the multifunctional fluorescent molecule comprising covalently bonded carbazole and anthracene moieties. J Mater Chem. 2011;21(25):9139-48.
[46] He J, Liu H, Dai Y, Ou X, Wang J, Tao S, et al. Nonconjugated Carbazoles: A Series of Novel Host Materials for Highly Efficient Blue Electrophosphorescent OLEDs. J Phys Chem C. 2009;113(16):6761-7.
[47] Kelkar AA, Patil NM, Chaudhari RV. Copper-catalyzed amination of aryl halides: single-step synthesis of triarylamines. Tetrahedron Lett. 2002;43(40):7143-6.
[48] Sarkar A, Chakravorti S. A solvent-dependent luminescence study on 9-phenyl carbazole. J Lumin. 1998;78(3):205-11.
[49] Tsai MH, Hong YH, Chang CH, Su HC, Wu CC, Matoliukstyte A, et al. 3-(9-Carbazolyl)carbazoles and 3,6-Di(9-carbazolyl)carbazoles as Effective Host Materials for Efficient Blue Organic Electrophosphorescence. Adv Mater. 2007;19(6):862-6.
[50] Berlman IB. Handbook of Fluorescence Spectra of Aromatic Molecules. Academic Press, Inc (London) 1971;2nd Ed.(United Kingdom).
[51] Costero AM, Sanchis J, Gil S, Sanz V, Williams JAG. Poly(amine) biphenyl derivatives as fluorescent sensors for anions and cations. J Mater Chem. 2005;15(27-28):2848-53.
[52] Arce R, Kevan L. Photochemical behaviour of N,N,N´,N´-tetramethylbenzidine and its protonated forms in sodium dodecyl sulphate anionic micelles under 337 nm laser irradiation. J Chem Soc, Faraday Trans 1: Phys Chem Condensed Phases. 1985;81(7):1669-76.
[53] Brunner K, van Dijken A, Börner H, Bastiaansen JJAM, Kiggen NMM, Langeveld BMW. Carbazole Compounds as Host Materials for Triplet Emitters in Organic Light-Emitting Diodes: Tuning the HOMO Level without Influencing the Triplet Energy in Small Molecules. J Am Chem Soc. 2004;126(19):6035-42.
[54] Robin MB, Day P. Mixed Valence Chemistry-A Survey and Classification. In: Emeléus HJ, Sharpe AG, editors. Advances in Inorganic Chemistry and Radiochemistry: Academic Press; 1968. p. 247-422.
[55] Crutchley RJ. Intervalence Charge Transfer and Electron Exchange Studies of Dinuclear Ruthenium Complexes. In: Sykes AG, editor. Advances in Inorganic Chemistry: Academic Press; 1994. p. 273-325.
[56] Seo ET, Nelson RF, Fritsch JM, Marcoux LS, Leedy DW, Adams RN. Anodic Oxidation Pathways of Aromatic Amines. Electrochemical and Electron Paramagnetic Resonance Studies. J Am Chem Soc. 1966;88(15):3498-503.
[57] Chiu KY, Su TX, Li JH, Lin T-H, Liou G-S, Cheng S-H. Novel trends of electrochemical oxidation of amino-substituted triphenylamine derivatives. J Electroanal Chem. 2005;575(1):95-101.
[58] Ramírez CL, Parise AR. Solvent resistant electrochromic polymer based on methylene-bridged arylamines. Org Electron. 2009;10(5):747-52.
[59] Chiu S-K, Chung Y-C, Liou G-S, Su YO. Electrochemical and Spectral Characterizations of 9-Phenylcarbazoles. J Chin Chem Soc. 2012;59(3):331-7.
[60] Xu B, Sheibani E, Liu P, Zhang J, Tian H, Vlachopoulos N, et al. Carbazole-Based Hole-Transport Materials for Efficient Solid-State Dye-Sensitized Solar Cells and Perovskite Solar Cells. Adv Mater. 2014;26(38):6629-34.

ACCEPTED MANUSCRIPT